

Determination of the Sign of the Decay Width Difference in the B_s^0 System

R. Aaij *et al.**

(LHCb Collaboration)

(Received 22 February 2012; published 11 June 2012)

The interference between the K^+K^- S -wave and P -wave amplitudes in $B_s^0 \rightarrow J/\psi K^+K^-$ decays with the K^+K^- pairs in the region around the $\phi(1020)$ resonance is used to determine the variation of the difference of the strong phase between these amplitudes as a function of K^+K^- invariant mass. Combined with the results from our CP asymmetry measurement in $B_s^0 \rightarrow J/\psi \phi$ decays, we conclude that the B_s^0 mass eigenstate that is almost $CP = +1$ is lighter and decays faster than the mass eigenstate that is almost $CP = -1$. This determines the sign of the decay width difference $\Delta\Gamma_s \equiv \Gamma_L - \Gamma_H$ to be positive. Our result also resolves the ambiguity in the past measurements of the CP violating phase ϕ_s to be close to zero rather than π . These conclusions are in agreement with the standard model expectations.

DOI: [10.1103/PhysRevLett.108.241801](https://doi.org/10.1103/PhysRevLett.108.241801)

PACS numbers: 14.40.Nd, 11.30.Er, 13.25.Hw

The decay time distributions of B_s^0 mesons decaying into the $J/\psi \phi$ final state have been used to measure the parameters ϕ_s and $\Delta\Gamma_s \equiv \Gamma_L - \Gamma_H$ of the B_s^0 system [1–3]. Here, ϕ_s is the CP violating phase equal to the phase difference between the amplitude for the direct decay and the amplitude for the decay after oscillation. Γ_L and Γ_H are the decay widths of the light and heavy B_s^0 mass eigenstates, respectively. The most precise results, presented recently by the LHCb experiment [3],

$$\begin{aligned} \phi_s &= 0.15 \pm 0.18 \text{ (stat)} \pm 0.06 \text{ (syst) rad,} \\ \Delta\Gamma_s &= 0.123 \pm 0.029 \text{ (stat)} \pm 0.011 \text{ (syst) ps}^{-1}, \end{aligned} \quad (1)$$

show no evidence of CP violation yet, indicating that CP violation is rather small in the B_s^0 system. There is clear evidence for the decay width difference $\Delta\Gamma_s$ being non-zero. It must be noted that there exists another solution,

$$\begin{aligned} \phi_s &= 2.99 \pm 0.18 \text{ (stat)} \pm 0.06 \text{ (syst) rad,} \\ \Delta\Gamma_s &= -0.123 \pm 0.029 \text{ (stat)} \pm 0.011 \text{ (syst) ps}^{-1}, \end{aligned} \quad (2)$$

arising from the fact that the time-dependent differential decay rates are invariant under the transformation $(\phi_s, \Delta\Gamma_s) \leftrightarrow (\pi - \phi_s, -\Delta\Gamma_s)$, together with an appropriate transformation for the strong phases. In the absence of CP violation, $\sin\phi_s = 0$, i.e., $\phi_s = 0$ or $\phi_s = \pi$, the two mass eigenstates also become CP eigenstates with $CP = +1$ and $CP = -1$, according to the relationship between B_s^0 mass eigenstates and CP eigenstates given in Ref. [4]. They can be identified by the decays into final states which are CP eigenstates. In $B_s^0 \rightarrow J/\psi K^+K^-$ decays, the final state is a superposition of $CP = +1$ and $CP = -1$ for the

K^+K^- pair in the P -wave configuration and $CP = -1$ for the K^+K^- pair in the S -wave configuration. Higher-order partial waves are neglected. These decays have different angular distributions of the final-state particles and are distinguishable.

Solution I is close to the case $\phi_s = 0$ and leads to the light (heavy) mass eigenstate being almost aligned with the $CP = +1$ ($CP = -1$) state. Similarly, solution II is close to the case $\phi_s = \pi$ and leads to the heavy (light) mass eigenstate being almost aligned with the $CP = +1$ ($CP = -1$) state. In Fig. 2 of Ref. [3], a fit to the observed decay time distribution shows that it can be well described by a superposition of two exponential functions corresponding to $CP = +1$ and $CP = -1$, compatible with no CP violation [3]. In this fit, the lifetime of the decay to the $CP = +1$ final state is found to be smaller than that of the decay to $CP = -1$. Thus, the mass eigenstate that is predominantly CP even decays faster than the CP odd state. For solution I, we find $\Delta\Gamma_s > 0$, i.e., $\Gamma_L > \Gamma_H$, and, for solution II, $\Delta\Gamma_s < 0$, i.e., $\Gamma_L < \Gamma_H$. In order to determine if the decay width difference $\Delta\Gamma_s$ is positive or negative, it is necessary to resolve the ambiguity between the two solutions.

Since each solution corresponds to a different set of strong phases, one may attempt to resolve the ambiguity by using the strong phases either as predicted by factorization or as measured in $B^0 \rightarrow J/\psi K^{*0}$ decays. Unfortunately, these two possibilities lead to opposite answers [5]. A direct experimental resolution of the ambiguity is therefore desirable.

In this Letter, we resolve this ambiguity using the decay $B_s^0 \rightarrow J/\psi K^+K^-$ with $J/\psi \rightarrow \mu^+\mu^-$. The total decay amplitude is a coherent sum of S -wave and P -wave contributions. The phase of the P -wave amplitude, which can be described by a spin-1 Breit-Wigner function of the invariant mass of the K^+K^- pair, denoted by m_{KK} , rises rapidly through the $\phi(1020)$ mass region. On the other hand, the phase of the S -wave amplitude should vary

*Full author list given at the end of the article.

relatively slowly for either an $f_0(980)$ contribution or a nonresonant contribution. As a result, the phase difference between the S -wave and P -wave amplitudes falls rapidly with increasing m_{KK} . By measuring this phase difference as a function of m_{KK} and taking the solution with a decreasing trend around the $\phi(1020)$ mass as the physical solution, the sign of $\Delta\Gamma_s$ is determined and the ambiguity in ϕ_s is resolved [6]. This is similar to the way the *BABAR* Collaboration measured the sign of $\cos 2\beta$ using the decay $B^0 \rightarrow J/\psi K_S^0 \pi^0$ [7], where 2β is the weak phase characterizing mixing-induced CP asymmetry in this decay.

The analysis is based on the same data sample as used in Ref. [3], which corresponds to an integrated luminosity of 0.37 fb^{-1} of pp collisions collected by the LHCb experiment at the Large Hadron Collider at the center-of-mass energy of $\sqrt{s} = 7 \text{ TeV}$. The LHCb detector is a forward spectrometer and is described in detail in Ref. [8]. The trigger, event selection criteria, and analysis method are very similar to those in Ref. [3], and here we discuss only the differences. The fraction of K^+K^- S -wave contribution measured within $\pm 12 \text{ MeV}$ of the nominal $\phi(1020)$ mass is $0.042 \pm 0.015 \pm 0.018$ [3]. (We adopt units such that $c = 1$ and $\hbar = 1$.) The S -wave fraction depends on the mass range taken around the $\phi(1020)$. The result of Ref. [3] is consistent with the CDF limit on the S -wave fraction of less than 6% at 95% C.L. (in the range 1009–1028 MeV) [2], smaller than the D0 result of $(12 \pm 3)\%$ (in 1010–1030 MeV) [9] and consistent with phenomenological expectations [10]. In order to apply the ambiguity resolution method described above, the range of m_{KK} is extended to 988–1050 MeV. Figure 1 shows the $\mu^+\mu^-K^+K^-$ mass distribution where the mass of the $\mu^+\mu^-$ pair is constrained to the nominal J/ψ mass. We perform an unbinned maximum likelihood fit to the invariant mass distribution of the selected B_s^0 candidates. The probability density function (PDF) for the signal B_s^0 invariant

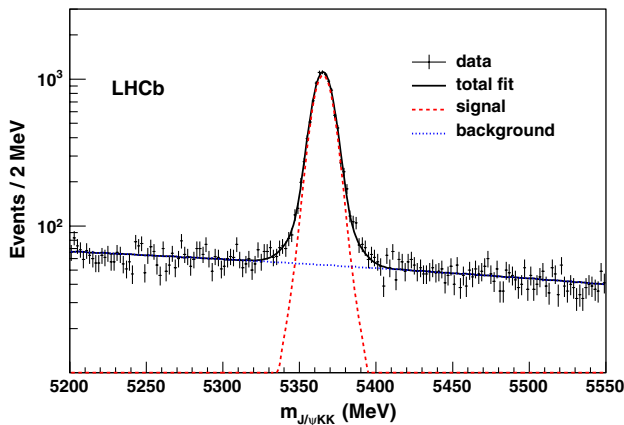


FIG. 1 (color online). Invariant mass distribution for $B_s^0 \rightarrow \mu^+\mu^-K^+K^-$ candidates, with the mass of the $\mu^+\mu^-$ pair constrained to the nominal J/ψ mass. The result of the fit is shown with signal (dashed curve) and combinatorial background (dotted curve) components and their sum (solid curve).

mass $m_{J/\psi KK}$ is modeled by two Gaussian functions with a common mean. The fraction of the wide Gaussian and its width relative to that of the narrow Gaussian is fixed to values obtained from simulated events. A linear function describes the $m_{J/\psi KK}$ distribution of the background, which is dominated by combinatorial background.

This analysis uses the sWeight technique [11] for background subtraction. The signal weight, denoted by $W_s(m_{J/\psi KK})$, is obtained using $m_{J/\psi KK}$ as the discriminating variable. The correlations between $m_{J/\psi KK}$ and other variables used in the analysis, including m_{KK} , decay time t , and the angular variables Ω defined in Ref. [3], are found to be negligible for both the signal and background components in the data. Figure 2 shows the m_{KK} distribution where the background is subtracted statistically using the sWeight technique. The range of m_{KK} is divided into four intervals: 988–1008, 1008–1020, 1020–1032, and 1032–1050 MeV. Table I gives the number of B_s^0 signal and background candidates in each interval.

In this analysis, we perform an unbinned maximum likelihood fit to the data using the sFit method [12], an extension of the sWeight technique, that simplifies fitting in the presence of background. In this method, it is only necessary to model the signal PDF, as background is canceled statistically using the signal weights.

The parameters of the $B_s^0 \rightarrow J/\psi K^+K^-$ decay time distribution are estimated from a simultaneous fit to the four intervals of m_{KK} by maximizing the log-likelihood function

$$\ln L(\Theta_P, \Theta_S) = \sum_{k=1}^4 W_{p;k} \sum_{i=1}^{N_k} W_s(m_{J/\psi KK;i}) \times \ln P_{\text{sig}}(t_i, \Omega_i, q_i, \omega_i; \Theta_P, \Theta_S),$$

where $N_k = N_{\text{sig};k} + N_{\text{bkg};k}$ is the number of candidates in the $m_{J/\psi KK}$ range of 5200–5550 MeV for the k th interval. Θ_P represents the physics parameters independent of m_{KK} ,

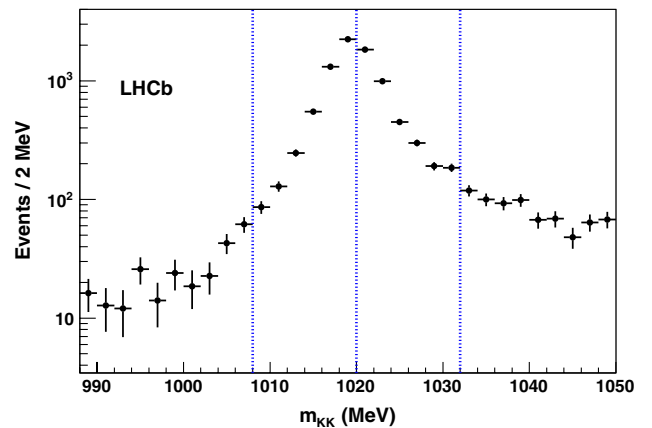


FIG. 2 (color online). Background subtracted K^+K^- invariant mass distribution for $B_s^0 \rightarrow J/\psi K^+K^-$ candidates. The vertical dash-dotted lines separate the four intervals.

TABLE I. Numbers of signal and background events in the $m_{J/\psi KK}$ range of 5200–5550 MeV and statistical power per signal event in four intervals of m_{KK} .

k	m_{KK} interval (MeV)	$N_{\text{sig};k}$	$N_{\text{bkg};k}$	$W_{p;k}$
1	988–1008	251 ± 21	1675 ± 43	0.700
2	1008–1020	4569 ± 70	2002 ± 49	0.952
3	1020–1032	3952 ± 66	2244 ± 51	0.938
4	1032–1050	726 ± 34	3442 ± 62	0.764

including ϕ_s , $\Delta\Gamma_s$, and the magnitudes and phases of the P -wave amplitudes. Note that the P -wave amplitudes for different polarizations share the same dependence on m_{KK} . Θ_S denotes the values of the m_{KK} -dependent parameters averaged over each interval, namely, the average fraction of S -wave contribution for the k th interval, $F_{S;k}$, and the average phase difference between the S -wave amplitude and the perpendicular P -wave amplitude for the k th interval, $\delta_{S\perp;k}$. P_{sig} is the signal PDF of the decay time t , angular variables Ω , initial flavor tag q , and the mistag probability ω . It is based on the theoretical differential decay rates [6] and includes experimental effects such as decay time resolution and acceptance, angular acceptance, and imperfect identification of the initial flavor of the B_s^0 particle, as described in Ref. [3]. The factors $W_{p;k}$ account for loss of statistical precision in parameter estimation due to background dilution and are necessary to obtain the correct error coverage. Their values are given in Table I.

The fit results for ϕ_s , $\Delta\Gamma_s$, $F_{S;k}$, and $\delta_{S\perp;k}$ are given in Table II. Figure 3 shows the estimated K^+K^- S -wave and P -wave contributions in the four m_{KK} intervals. The shape of the measured P -wave m_{KK} distribution is in good agreement with that of $B_s^0 \rightarrow J/\psi\phi$ events simulated using a spin-1 relativistic Breit-Wigner function for the $\phi(1020)$ amplitude. In Fig. 4, the phase difference between the S -wave and the perpendicular P -wave amplitude is plotted in four m_{KK} intervals for solution I and solution II.

TABLE II. Results from a simultaneous fit of the four intervals of m_{KK} , where the uncertainties are statistical only. Only parameters which are needed for the ambiguity resolution are shown.

Parameter	Solution I	Solution II
ϕ_s (rad)	0.167 ± 0.175	2.975 ± 0.175
$\Delta\Gamma$ (ps^{-1})	0.120 ± 0.028	-0.120 ± 0.028
$F_{S;1}$	0.283 ± 0.113	0.283 ± 0.113
$F_{S;2}$	0.061 ± 0.022	0.061 ± 0.022
$F_{S;3}$	0.044 ± 0.022	0.044 ± 0.022
$F_{S;4}$	0.269 ± 0.067	0.269 ± 0.067
$\delta_{S\perp;1}$ (rad)	$2.68^{+0.35}_{-0.42}$	$0.46^{+0.42}_{-0.35}$
$\delta_{S\perp;2}$ (rad)	$0.22^{+0.15}_{-0.13}$	$2.92^{+0.13}_{-0.15}$
$\delta_{S\perp;3}$ (rad)	$-0.11^{+0.16}_{-0.18}$	$3.25^{+0.18}_{-0.16}$
$\delta_{S\perp;4}$ (rad)	$-0.97^{+0.28}_{-0.43}$	$4.11^{+0.43}_{-0.28}$

Figure 4 shows a clear decreasing trend of the phase difference between the S -wave and P -wave amplitudes in the $\phi(1020)$ mass region for solution I, as expected for the physical solution. To estimate the significance of the result, we perform an unbinned maximum likelihood fit to the data by parametrizing the phase difference $\delta_{S\perp;k}$ as a linear function of the average m_{KK} value in the k th interval. This leads to a slope of $-0.050^{+0.013}_{-0.020}$ rad/MeV for solution I and the opposite sign for solution II, where the uncertainties are statistical only. The difference of the $\ln L$ value between this fit and a fit in which the slope is fixed to be zero is 11.0. Hence, the negative trend of solution I has a significance of 4.7 standard deviations. Therefore, we conclude that solution I, which has $\Delta\Gamma_s > 0$, is the physical solution. The trend of solution I is also qualitatively consistent with that of the phase difference between the K^+K^- S -wave and P -wave amplitudes versus m_{KK} measured in the decay $D_s^+ \rightarrow K^+K^-\pi^+$ by the BABAR Collaboration [13].

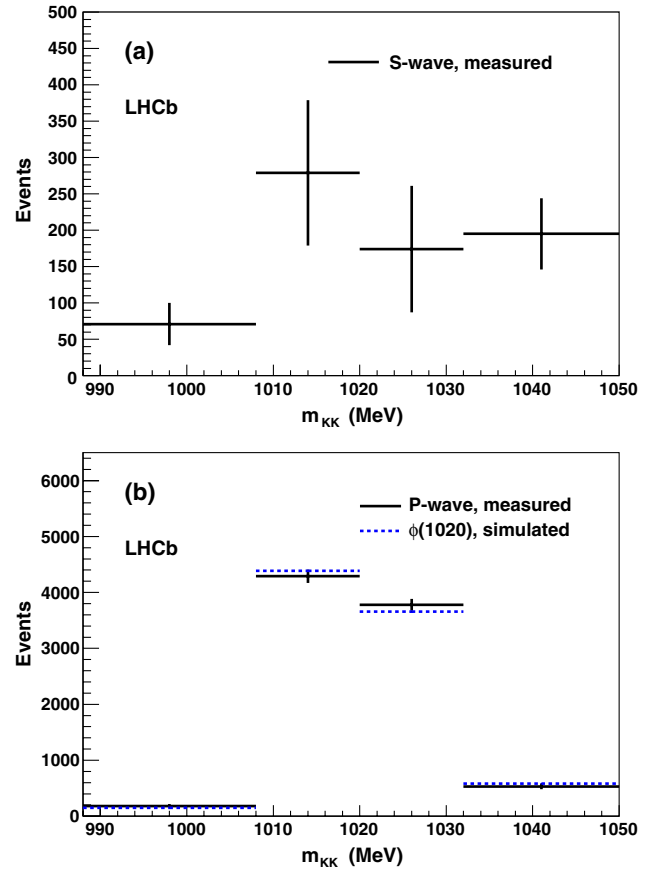


FIG. 3 (color online). Distribution of (a) K^+K^- S -wave signal events and (b) K^+K^- P -wave signal events, both in four invariant mass intervals. In (b), the distribution of simulated $B_s^0 \rightarrow J/\psi\phi$ events in the four intervals assuming the same total number of P -wave events is also shown (dashed lines). Note that the interference between the K^+K^- S -wave and P -wave amplitudes integrated over the angular variables has a vanishing contribution in these distributions.

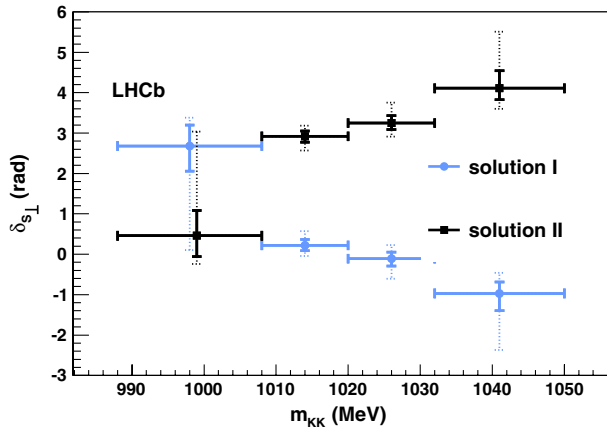


FIG. 4 (color online). Measured phase differences between S -wave and perpendicular P -wave amplitudes in four intervals of m_{KK} for solution I (full blue circles) and solution II (full black squares). The asymmetric error bars correspond to $\Delta \ln L = -0.5$ (solid lines) and $\Delta \ln L = -2$ (dash-dotted lines).

Several possible sources of systematic uncertainty on the phase variation versus m_{KK} have been considered. A possible background from decays with similar final states such as $B^0 \rightarrow J/\psi K^{*0}$ could have a small effect. From simulation, the contamination to the signal from such decays is estimated to be 1.1% in the m_{KK} range of 988–1050 MeV. We add a 2.2% contribution of simulated $B^0 \rightarrow J/\psi K^{*0}$ events to the data and repeat the analysis. The largest observed change is a shift of $\delta_{S\perp,4}$ by 0.06 rad, which is only 20% of its statistical uncertainty and has a negligible effect on the slope of $\delta_{S\perp}$ versus m_{KK} . The effect of neglecting the variation of the values of F_S and $\delta_{S\perp}$ in each m_{KK} interval is determined to change the significance of the negative trend of solution I by less than 0.1 standard deviations. We also repeat the analysis for different m_{KK} ranges, different ways of dividing the m_{KK} range, or different shapes of the signal and background $m_{J/\psi KK}$ distributions. The significance of the negative trend of solution I is not affected. To measure precisely the S -wave line shape and determine its resonance structure, more data are needed. However, the results presented here do not depend on such detailed knowledge.

In conclusion, the analysis of the strong interaction phase shift resolves the ambiguity between solution I and solution II. Values of ϕ_s close to zero and positive $\Delta\Gamma_s$ are preferred. It follows that, in the B_s^0 system, the mass

eigenstate that is almost CP even is lighter and decays faster than the state that is almost CP odd. This is in agreement with the standard model expectations (e.g., [14]). It is also interesting to note that this situation is similar to that in the neutral kaon system.

We express our gratitude to our colleagues in the CERN accelerator departments for the excellent performance of the LHC. We thank the technical and administrative staff at CERN and at the LHCb institutes and acknowledge support from the National Agencies: CAPES, CNPq, FAPERJ, and FINEP (Brazil); CERN; NSFC (China); CNRS/IN2P3 (France); BMBF, DFG, HGF, and MPG (Germany); SFI (Ireland); INFN (Italy); FOM and NWO (The Netherlands); SCSR (Poland); ANCS (Romania); MinES of Russia and Rosatom (Russia); MICINN, XuntaGal, and GENCAT (Spain); SNSF and SER (Switzerland); NAS Ukraine (Ukraine); STFC (United Kingdom); and NSF (USA). We also acknowledge the support received from the ERC under FP7 and the Region Auvergne.

-
- [1] V.M. Abazov *et al.* (D0 Collaboration), *Phys. Rev. D* **85**, 032006 (2012).
 - [2] T. Aaltonen *et al.* (CDF Collaboration), [arXiv:1112.1726](https://arxiv.org/abs/1112.1726).
 - [3] R. Aaij *et al.* (LHCb Collaboration), *Phys. Rev. Lett.* **108**, 101803 (2012).
 - [4] I. Dunietz, R. Fleischer, and U. Nierste, *Phys. Rev. D* **63**, 114015 (2001).
 - [5] S. Nandi and U. Nierste, *Phys. Rev. D* **77**, 054010 (2008).
 - [6] Y. Xie, P. Clarke, G. Cowan, and F. Muheim, *J. High Energy Phys.* **09** (2009) 074.
 - [7] B. Aubert *et al.* (BABAR Collaboration), *Phys. Rev. D* **71**, 032005 (2005).
 - [8] A. A. Alves *et al.* (LHCb Collaboration), *JINST* **3**, S08005 (2008).
 - [9] V.M. Abazov *et al.* (D0 Collaboration), *Phys. Rev. D* **85**, 011103 (2012).
 - [10] S. Stone and L. Zhang, *Phys. Rev. D* **79**, 074024 (2009).
 - [11] M. Pivk and F.R. Le Diberder, *Nucl. Instrum. Methods Phys. Res., Sect. A* **555**, 356 (2005).
 - [12] Y. Xie, [arXiv:0905.0724](https://arxiv.org/abs/0905.0724).
 - [13] P. del Amo Sanchez *et al.* (BABAR Collaboration), *Phys. Rev. D* **83**, 052001 (2011).
 - [14] A. Lenz, U. Nierste, J. Charles, S. Descotes-Genon, A. Jantsch, C. Kaufhold, H. Lacker, S. Monteil, V. Niess, and S. T'Jampens, *Phys. Rev. D* **83**, 036004 (2011).

R. Aaij,³⁸ C. Abellan Beteta,^{33,n} B. Adeva,³⁴ M. Adinolfi,⁴³ C. Adrover,⁶ A. Affolder,⁴⁹ Z. Ajaltouni,⁵ J. Albrecht,³⁵ F. Alessio,³⁵ M. Alexander,⁴⁸ G. Alkhazov,²⁷ P. Alvarez Cartelle,³⁴ A. A. Alves, Jr.,²² S. Amato,² Y. Amhis,³⁶ J. Anderson,³⁷ R. B. Appleby,⁵¹ O. Aquines Gutierrez,¹⁰ F. Archilli,^{18,35} L. Arrabito,⁵⁵ A. Artamonov,³² M. Artuso,^{53,35} E. Aslanides,⁶ G. Auriemma,^{22,m} S. Bachmann,¹¹ J. J. Back,⁴⁵ D. S. Bailey,⁵¹ V. Balagura,^{28,35} W. Baldini,¹⁶ R. J. Barlow,⁵¹ C. Barschel,³⁵ S. Barsuk,⁷ W. Barter,⁴⁴ A. Bates,⁴⁸ C. Bauer,¹⁰ Th. Bauer,³⁸ A. Bay,³⁶ I. Bediaga,¹ S. Belogurov,²⁸ K. Belous,³² I. Belyaev,²⁸ E. Ben-Haim,⁸ M. Benayoun,⁸ G. Bencivenni,¹⁸ S. Benson,⁴⁷ J. Benton,⁴³ R. Bernet,³⁷ M.-O. Bettler,¹⁷ M. van Beuzekom,³⁸ A. Bien,¹¹ S. Bifani,¹² T. Bird,⁵¹ A. Bizzeti,^{17,h}

P. M. Bjørnstad,⁵¹ T. Blake,³⁵ F. Blanc,³⁶ C. Blanks,⁵⁰ J. Blouw,¹¹ S. Blusk,⁵³ A. Bobrov,³¹ V. Bocci,²² A. Bondar,³¹ N. Bondar,²⁷ W. Bonivento,¹⁵ S. Borghi,^{48,51} A. Borgia,⁵³ T. J. V. Bowcock,⁴⁹ C. Bozzi,¹⁶ T. Brambach,⁹ J. van den Brand,³⁹ J. Bressieux,³⁶ D. Brett,⁵¹ M. Britsch,¹⁰ T. Britton,⁵³ N. H. Brook,⁴³ H. Brown,⁴⁹ K. de Bruyn,³⁸ A. Büchler-Germann,³⁷ I. Burducea,²⁶ A. Bursche,³⁷ J. Buytaert,³⁵ S. Cadeddu,¹⁵ O. Callot,⁷ M. Calvi,^{20,j} M. Calvo Gomez,^{33,n} A. Camboni,³³ P. Campana,^{18,35} A. Carbone,¹⁴ G. Carboni,^{21,k} R. Cardinale,^{19,35,i} A. Cardini,¹⁵ L. Carson,⁵⁰ K. Carvalho Akiba,² G. Casse,⁴⁹ M. Cattaneo,³⁵ Ch. Cauet,⁹ M. Charles,⁵² Ph. Charpentier,³⁵ N. Chiapolini,³⁷ K. Ciba,³⁵ X. Cid Vidal,³⁴ G. Ciezarek,⁵⁰ P. E. L. Clarke,^{47,35} M. Clemencic,³⁵ H. V. Cliff,⁴⁴ J. Closier,³⁵ C. Coca,²⁶ V. Coco,³⁸ J. Cogan,⁶ P. Collins,³⁵ A. Comerma-Montells,³³ F. Constantin,²⁶ A. Contu,⁵² A. Cook,⁴³ M. Coombes,⁴³ G. Corti,³⁵ B. Couturier,³⁵ G. A. Cowan,³⁶ R. Currie,⁴⁷ C. D'Ambrosio,³⁵ P. David,⁸ P. N. Y. David,³⁸ I. De Bonis,⁴ S. De Capua,^{21,k} M. De Cian,³⁷ F. De Lorenzi,¹² J. M. De Miranda,¹ L. De Paula,² P. De Simone,¹⁸ D. Decamp,⁴ M. Deckenhoff,⁹ H. Degaudenzi,^{36,35} L. Del Buono,⁸ C. Deplano,¹⁵ D. Derkach,^{14,35} O. Deschamps,⁵ F. Dettori,³⁹ J. Dickens,⁴⁴ H. Dijkstra,³⁵ P. Diniz Batista,¹ F. Domingo Bonal,^{33,n} S. Donleavy,⁴⁹ F. Dordei,¹¹ A. Dosil Suárez,³⁴ D. Dossett,⁴⁵ A. Dovbnya,⁴⁰ F. Dupertuis,³⁶ R. Dzhelyadin,³² A. Dziurda,²³ S. Easo,⁴⁶ U. Egede,⁵⁰ V. Egorychev,²⁸ S. Eidelman,³¹ D. van Eijk,³⁸ F. Eisele,¹¹ S. Eisenhardt,⁴⁷ R. Ekelhof,⁹ L. Eklund,⁴⁸ Ch. Elsasser,³⁷ D. Elsby,⁴² D. Esperante Pereira,³⁴ A. Falabella,^{16,14,e} E. Fanchini,^{20,j} C. Färber,¹¹ G. Fardell,⁴⁷ C. Farinelli,³⁸ S. Farry,¹² V. Fave,³⁶ V. Fernandez Albor,³⁴ M. Ferro-Luzzi,³⁵ S. Filippov,³⁰ C. Fitzpatrick,⁴⁷ M. Fontana,¹⁰ F. Fontanelli,^{19,i} R. Forty,³⁵ O. Francisco,² M. Frank,³⁵ C. Frei,³⁵ M. Frosini,^{17,f} S. Furcas,²⁰ A. Gallas Torreira,³⁴ D. Galli,^{14,c} M. Gandelman,² P. Gandini,⁵² Y. Gao,³ J.-C. Garnier,³⁵ J. Garofoli,⁵³ J. Garra Tico,⁴⁴ L. Garrido,³³ D. Gascon,³³ C. Gaspar,³⁵ R. Gauld,⁵² N. Gauvin,³⁶ M. Gersabeck,³⁵ T. Gershon,^{45,35} Ph. Ghez,⁴ V. Gibson,⁴⁴ V. V. Gligorov,³⁵ C. Göbel,⁵⁴ D. Golubkov,²⁸ A. Golutvin,^{50,28,35} A. Gomes,² H. Gordon,⁵² M. Grabalosa Gándara,³³ R. Graciani Diaz,³³ L. A. Granado Cardoso,³⁵ E. Graugés,³³ G. Graziani,¹⁷ A. Greco,²⁶ E. Greening,⁵² S. Gregson,⁴⁴ B. Gui,⁵³ E. Gushchin,³⁰ Yu. Guz,³² T. Gys,³⁵ C. Hadjivasiliou,⁵³ G. Haefeli,³⁶ C. Haen,³⁵ S. C. Haines,⁴⁴ T. Hampson,⁴³ S. Hansmann-Menzemer,¹¹ R. Harji,⁵⁰ N. Harnew,⁵² J. Harrison,⁵¹ P. F. Harrison,⁴⁵ T. Hartmann,⁵⁶ J. He,⁷ V. Heijne,³⁸ K. Hennessy,⁴⁹ P. Henrard,⁵ J. A. Hernando Morata,³⁴ E. van Herwijnen,³⁵ E. Hicks,⁴⁹ K. Holubyev,¹¹ P. Hopchev,⁴ W. Hulsbergen,³⁸ P. Hunt,⁵² T. Huse,⁴⁹ R. S. Huston,¹² D. Hutchcroft,⁴⁹ D. Hynds,⁴⁸ V. Iakovenko,⁴¹ P. Ilten,¹² J. Imong,⁴³ R. Jacobsson,³⁵ A. Jaeger,¹¹ M. Jahjah Hussein,⁵ E. Jans,³⁸ F. Jansen,³⁸ P. Jaton,³⁶ B. Jean-Marie,⁷ F. Jing,³ M. John,⁵² D. Johnson,⁵² C. R. Jones,⁴⁴ B. Jost,³⁵ M. Kaballo,⁹ S. Kandybei,⁴⁰ M. Karacson,³⁵ T. M. Karbach,⁹ J. Keaveney,¹² I. R. Kenyon,⁴² U. Kerzel,³⁵ T. Ketel,³⁹ A. Keune,³⁶ B. Khanji,⁶ Y. M. Kim,⁴⁷ M. Knecht,³⁶ R. F. Koopman,³⁹ P. Koppenburg,³⁸ M. Korolev,²⁹ A. Kozlinskiy,³⁸ L. Kravchuk,³⁰ K. Kreplin,¹¹ M. Kreps,⁴⁵ G. Krocker,¹¹ P. Krokovny,¹¹ F. Kruse,⁹ K. Kruszelecki,³⁵ M. Kucharczyk,^{20,23,35,j} T. Kvaratskheliya,^{28,35} V. N. La Thi,³⁶ D. Lacarrere,³⁵ G. Lafferty,⁵¹ A. Lai,¹⁵ D. Lambert,⁴⁷ R. W. Lambert,³⁹ E. Lanciotti,³⁵ G. Lanfranchi,¹⁸ C. Langenbruch,¹¹ T. Latham,⁴⁵ C. Lazzeroni,⁴² R. Le Gac,⁶ J. van Leerdam,³⁸ J.-P. Lees,⁴ R. Lefèvre,⁵ A. Leflat,^{29,35} J. Lefrançois,⁷ O. Leroy,⁶ T. Lesiak,²³ L. Li,³ L. Li Gioi,⁵ M. Lieng,⁹ M. Liles,⁴⁹ R. Lindner,³⁵ C. Linn,¹¹ B. Liu,³ G. Liu,³⁵ J. von Loeben,²⁰ J. H. Lopes,² E. Lopez Asamar,³³ N. Lopez-March,³⁶ H. Lu,³ J. Luisier,³⁶ A. Mac Raighne,⁴⁸ F. Machefert,⁷ I. V. Machikhiliyan,^{4,28} F. Maciuc,¹⁰ O. Maev,^{27,35} J. Magnin,¹ S. Malde,⁵² R. M. D. Mamunur,³⁵ G. Manca,^{15,d} G. Mancinelli,⁶ N. Mangiafave,⁴⁴ U. Marconi,¹⁴ R. Märki,³⁶ J. Marks,¹¹ G. Martellotti,²² A. Martens,⁸ L. Martin,⁵² A. Martín Sánchez,⁷ D. Martinez Santos,³⁵ A. Massafferri,¹ Z. Mathe,¹² C. Matteuzzi,²⁰ M. Matveev,²⁷ E. Maurice,⁶ B. Maynard,⁵³ A. Mazurov,^{16,30,35} G. McGregor,⁵¹ R. McNulty,¹² M. Meissner,¹¹ M. Merk,³⁸ J. Merkel,⁹ R. Messi,^{21,k} S. Miglioranzi,³⁵ D. A. Milanes,¹³ M.-N. Minard,⁴ J. Molina Rodriguez,⁵⁴ S. Monteil,⁵ D. Moran,¹² P. Morawski,²³ R. Mountain,⁵³ I. Mous,³⁸ F. Muheim,⁴⁷ K. Müller,³⁷ R. Muresan,²⁶ B. Muryn,²⁴ B. Muster,³⁶ M. Musy,³³ J. Mylroie-Smith,⁴⁹ P. Naik,⁴³ T. Nakada,³⁶ R. Nandakumar,⁴⁶ I. Nasteva,¹ M. Nedos,⁹ M. Needham,⁴⁷ N. Neufeld,³⁵ A. D. Nguyen,³⁶ C. Nguyen-Mau,^{36,o} M. Nicol,⁷ V. Niess,⁵ N. Nikitin,²⁹ A. Nomerotski,^{52,35} A. Novoselov,³² A. Oblakowska-Mucha,²⁴ V. Obraztsov,³² S. Oggero,³⁸ S. Ogilvy,⁴⁸ O. Okhrimenko,⁴¹ R. Oldeman,^{15,35,d} M. Orlandea,²⁶ J. M. Otalora Goicochea,² P. Owen,⁵⁰ K. Pal,⁵³ J. Palacios,³⁷ A. Palano,^{13,b} M. Palutan,¹⁸ J. Panman,³⁵ A. Papanestis,⁴⁶ M. Pappagallo,⁴⁸ C. Parkes,⁵¹ C. J. Parkinson,⁵⁰ G. Passaleva,¹⁷ G. D. Patel,⁴⁹ M. Patel,⁵⁰ S. K. Paterson,⁵⁰ G. N. Patrick,⁴⁶ C. Patrignani,^{19,i} C. Pavel-Nicorescu,²⁶ A. Pazos Alvarez,³⁴ A. Pellegrino,³⁸ G. Penso,^{22,1} M. Pepe Altarelli,³⁵ S. Perazzini,^{14,c} D. L. Perego,^{20,j} E. Perez Trigo,³⁴ A. Pérez-Calero Yzquierdo,³³ P. Perret,⁵ M. Perrin-Terrin,⁶ G. Pessina,²⁰ A. Petrella,^{16,35} A. Petrolini,^{19,i} A. Phan,⁵³ E. Picatoste Olloqui,³³ B. Pie Valls,³³ B. Pietrzyk,⁴ T. Pilarč,⁴⁵ D. Pinci,²² R. Plackett,⁴⁸ S. Playfer,⁴⁷ M. Plo Casasus,³⁴ G. Polok,²³ A. Poluektov,^{45,31} E. Polycarpo,² D. Popov,¹⁰ B. Popovici,²⁶ C. Potterat,³³ A. Powell,⁵²

J. Prisciandaro,³⁶ V. Pugatch,⁴¹ A. Puig Navarro,³³ W. Qian,⁵³ J.H. Rademacker,⁴³ B. Rakotomiaramanana,³⁶ M. S. Rangel,² I. Raniuk,⁴⁰ G. Raven,³⁹ S. Redford,⁵² M. M. Reid,⁴⁵ A. C. dos Reis,¹ S. Ricciardi,⁴⁶ A. Richards,⁵⁰ K. Rinnert,⁴⁹ D. A. Roa Romero,⁵ P. Robbe,⁷ E. Rodrigues,^{48,51} F. Rodrigues,² P. Rodriguez Perez,³⁴ G. J. Rogers,⁴⁴ S. Roiser,³⁵ V. Romanovsky,³² M. Rosello,^{33,n} J. Rouvinet,³⁶ T. Ruf,³⁵ H. Ruiz,³³ G. Sabatino,^{21,k} J. J. Saborido Silva,³⁴ N. Sagidova,²⁷ P. Sail,⁴⁸ B. Saitta,^{15,d} C. Salzmann,³⁷ M. Sannino,^{19,i} R. Santacesaria,²² C. Santamarina Rios,³⁴ R. Santinelli,³⁵ E. Santovetti,^{21,k} M. Sapunov,⁶ A. Sarti,^{18,l} C. Satriano,^{22,m} A. Satta,²¹ M. Savrie,^{16,e} D. Savrina,²⁸ P. Schaack,⁵⁰ M. Schiller,³⁹ S. Schleich,⁹ M. Schlupp,⁹ M. Schmelling,¹⁰ B. Schmidt,³⁵ O. Schneider,³⁶ A. Schopper,³⁵ M.-H. Schune,⁷ R. Schwemmer,³⁵ B. Sciascia,¹⁸ A. Sciubba,^{18,l} M. Seco,³⁴ A. Semennikov,²⁸ K. Senderowska,²⁴ I. Sepp,⁵⁰ N. Serra,³⁷ J. Serrano,⁶ P. Seyfert,¹¹ M. Shapkin,³² I. Shapoval,^{40,35} P. Shatalov,²⁸ Y. Shcheglov,²⁷ T. Shears,⁴⁹ L. Shekhtman,³¹ O. Shevchenko,⁴⁰ V. Shevchenko,²⁸ A. Shires,⁵⁰ R. Silva Coutinho,⁴⁵ T. Skwarnicki,⁵³ N. A. Smith,⁴⁹ E. Smith,^{52,46} K. Sobczak,⁵ F. J. P. Soler,⁴⁸ A. Solomin,⁴³ F. Soomro,^{18,35} B. Souza De Paula,² B. Spaan,⁹ A. Sparkes,⁴⁷ P. Spradlin,⁴⁸ F. Stagni,³⁵ S. Stahl,¹¹ O. Steinkamp,³⁷ S. Stoica,²⁶ S. Stone,^{53,35} B. Storaci,³⁸ M. Straticiuc,²⁶ U. Straumann,³⁷ V. K. Subbiah,³⁵ S. Swientek,⁹ M. Szczekowski,²⁵ P. Szczypka,³⁶ T. Szumlak,²⁴ S. T'Jampens,⁴ E. Teodorescu,²⁶ F. Teubert,³⁵ C. Thomas,⁵² E. Thomas,³⁵ J. van Tilburg,¹¹ V. Tisserand,⁴ M. Tobin,³⁷ S. Topp-Joergensen,⁵² N. Torr,⁵² E. Tournefier,^{4,50} S. Tourneur,³⁶ M. T. Tran,³⁶ A. Tsaregorodtsev,⁶ N. Tuning,³⁸ M. Ubeda Garcia,³⁵ A. Ukleja,²⁵ P. Urquijo,⁵³ U. Uwer,¹¹ V. Vagnoni,¹⁴ G. Valenti,¹⁴ R. Vazquez Gomez,³³ P. Vazquez Regueiro,³⁴ S. Vecchi,¹⁶ J. J. Velthuis,⁴³ M. Veltri,^{17,g} B. Viaud,⁷ I. Videau,⁷ D. Vieira,² X. Vilasis-Cardona,^{33,n} J. Visniakov,³⁴ A. Vollhardt,³⁷ D. Volyanskyy,¹⁰ D. Voong,⁴³ A. Vorobyev,²⁷ H. Voss,¹⁰ S. Wandernoth,¹¹ J. Wang,⁵³ D. R. Ward,⁴⁴ N. K. Watson,⁴² A. D. Webber,⁵¹ D. Websdale,⁵⁰ M. Whitehead,⁴⁵ D. Wiedner,¹¹ L. Wiggers,³⁸ G. Wilkinson,⁵² M. P. Williams,^{45,46} M. Williams,⁵⁰ F. F. Wilson,⁴⁶ J. Wishahi,⁹ M. Witek,²³ W. Witzeling,³⁵ S. A. Wotton,⁴⁴ K. Wyllie,³⁵ Y. Xie,⁴⁷ F. Xing,⁵² Z. Xing,⁵³ Z. Yang,³ R. Young,⁴⁷ O. Yushchenko,³² M. Zangoli,¹⁴ M. Zavertyaev,^{10,a} F. Zhang,³ L. Zhang,⁵³ W. C. Zhang,¹² Y. Zhang,³ A. Zhelezov,¹¹ L. Zhong,³ and A. Zvyagin³⁵

(LHCb Collaboration)

¹Centro Brasileiro de Pesquisas Físicas (CBPF), Rio de Janeiro, Brazil²Universidade Federal do Rio de Janeiro (UFRJ), Rio de Janeiro, Brazil³Center for High Energy Physics, Tsinghua University, Beijing, China⁴LAPP, Université de Savoie, CNRS/IN2P3, Annecy-Le-Vieux, France⁵Clermont Université, Université Blaise Pascal, CNRS/IN2P3, LPC, Clermont-Ferrand, France⁶CPPM, Aix-Marseille Université, CNRS/IN2P3, Marseille, France⁷LAL, Université Paris-Sud, CNRS/IN2P3, Orsay, France⁸LPNHE, Université Pierre et Marie Curie, Université Paris Diderot, CNRS/IN2P3, Paris, France⁹Fakultät Physik, Technische Universität Dortmund, Dortmund, Germany¹⁰Max-Planck-Institut für Kernphysik (MPIK), Heidelberg, Germany¹¹Physikalisches Institut, Ruprecht-Karls-Universität Heidelberg, Heidelberg, Germany¹²School of Physics, University College Dublin, Dublin, Ireland¹³Sezione INFN di Bari, Bari, Italy¹⁴Sezione INFN di Bologna, Bologna, Italy¹⁵Sezione INFN di Cagliari, Cagliari, Italy¹⁶Sezione INFN di Ferrara, Ferrara, Italy¹⁷Sezione INFN di Firenze, Firenze, Italy¹⁸Laboratori Nazionali dell'INFN di Frascati, Frascati, Italy¹⁹Sezione INFN di Genova, Genova, Italy²⁰Sezione INFN di Milano Bicocca, Milano, Italy²¹Sezione INFN di Roma Tor Vergata, Roma, Italy²²Sezione INFN di Roma La Sapienza, Roma, Italy²³Henryk Niewodniczanski Institute of Nuclear Physics, Polish Academy of Sciences, Kraków, Poland²⁴AGH University of Science and Technology, Kraków, Poland²⁵Soltan Institute for Nuclear Studies, Warsaw, Poland²⁶Horia Hulubei National Institute of Physics and Nuclear Engineering, Bucharest-Magurele, Romania²⁷Petersburg Nuclear Physics Institute (PNPI), Gatchina, Russia²⁸Institute of Theoretical and Experimental Physics (ITEP), Moscow, Russia²⁹Institute of Nuclear Physics, Moscow State University (SINP MSU), Moscow, Russia³⁰Institute for Nuclear Research of the Russian Academy of Sciences (INR RAS), Moscow, Russia

- ³¹*Budker Institute of Nuclear Physics (SB RAS) and Novosibirsk State University, Novosibirsk, Russia*
³²*Institute for High Energy Physics (IHEP), Protvino, Russia*
³³*Universitat de Barcelona, Barcelona, Spain*
³⁴*Universidad de Santiago de Compostela, Santiago de Compostela, Spain*
³⁵*European Organization for Nuclear Research (CERN), Geneva, Switzerland*
³⁶*Ecole Polytechnique Fédérale de Lausanne (EPFL), Lausanne, Switzerland*
³⁷*Physik-Institut, Universität Zürich, Zürich, Switzerland*
³⁸*Nikhef National Institute for Subatomic Physics, Amsterdam, The Netherlands*
³⁹*Nikhef National Institute for Subatomic Physics and Vrije Universiteit, Amsterdam, The Netherlands*
⁴⁰*NSC Kharkiv Institute of Physics and Technology (NSC KIPT), Kharkiv, Ukraine*
⁴¹*Institute for Nuclear Research of the National Academy of Sciences (KINR), Kyiv, Ukraine*
⁴²*University of Birmingham, Birmingham, United Kingdom*
⁴³*H. H. Wills Physics Laboratory, University of Bristol, Bristol, United Kingdom*
⁴⁴*Cavendish Laboratory, University of Cambridge, Cambridge, United Kingdom*
⁴⁵*Department of Physics, University of Warwick, Coventry, United Kingdom*
⁴⁶*STFC Rutherford Appleton Laboratory, Didcot, United Kingdom*
⁴⁷*School of Physics and Astronomy, University of Edinburgh, Edinburgh, United Kingdom*
⁴⁸*School of Physics and Astronomy, University of Glasgow, Glasgow, United Kingdom*
⁴⁹*Oliver Lodge Laboratory, University of Liverpool, Liverpool, United Kingdom*
⁵⁰*Imperial College London, London, United Kingdom*
⁵¹*School of Physics and Astronomy, University of Manchester, Manchester, United Kingdom*
⁵²*Department of Physics, University of Oxford, Oxford, United Kingdom*
⁵³*Syracuse University, Syracuse, New York, USA*
⁵⁴*Pontifícia Universidade Católica do Rio de Janeiro (PUC-Rio), Rio de Janeiro, Brazil*
⁵⁵*CC-IN2P3, CNRS/IN2P3, Lyon-Villeurbanne, France*
⁵⁶*Physikalisches Institut, Universität Rostock, Rostock, Germany*

^aAlso at P.N. Lebedev Physical Institute, Russian Academy of Sciences (LPI RAS), Moscow, Russia.

^bAlso at Università di Bari, Bari, Italy.

^cAlso at Università di Bologna, Bologna, Italy.

^dAlso at Università di Cagliari, Cagliari, Italy.

^eAlso at Università di Ferrara, Ferrara, Italy.

^fAlso at Università di Firenze, Firenze, Italy.

^gAlso at Università di Urbino, Urbino, Italy.

^hAlso at Università di Modena e Reggio Emilia, Modena, Italy.

ⁱAlso at Università di Genova, Genova, Italy.

^jAlso at Università di Milano Bicocca, Milano, Italy.

^kAlso at Università di Roma Tor Vergata, Roma, Italy.

^lAlso at Università di Roma La Sapienza, Roma, Italy.

^mAlso at Università della Basilicata, Potenza, Italy.

ⁿAlso at LIFAELS, La Salle, Universitat Ramon Llull, Barcelona, Spain.

^oAlso at Hanoi University of Science, Hanoi, Vietnam.